Pollutant dispersion in a group of courtyard buildings

Simone Ferrari[1*]

[1]DICAAR - Dipartimento di Ingegneria Civile, Ambientale e Architettura, University of Cagliari, via Marengo 2, 09123 Cagliari, Italy

Abstract. As stated by the World Health Organization (WHO), the air pollution in the urban environment is the silent cause for around seven million death worldwide. This is due to the indoor and outdoor exposure to various pollutants emitted in the built environment: as the global trend is an increase of the population living in towns, this issue is predicted to become even worser. As a matter of fact, the built environment can cause the trapping of pollutants instead of their dispersion. In this work, the dispersion of a plume of a pollutant (carbon monoxide, CO), emitted from a chimneystack above the roof of courtyard in a group of courtyards, is investigated. This is achieved employing the ENVI-met software, able to model, among the others, the turbulence and pollutant dispersion in the built environment. Results show, among the others, how the pollutant emitted from an upstream building can harm also the downstream buildings.

1 Introduction

The 2021 report of the United Nations' World Health Organization (WHO) [1] has taken to the world attention the issue of the urban air pollution, with the majority of world population living in the most polluted areas, the cities (55% of the world population lives in urban areas, according to the UN, with a perspective of increase of this percentage to 68% by 2050 [2]). As a matter of fact, the urban air pollution has been recalled as the silent killer causing around seven million deaths worldwide, due to air pollution related causes, from polluted air over the cities to the smoke inside houses. Moreover, WHO estimates that almost all the global population (around 99%) is exposed to such a level of air pollution to encounter an increased risk for dangerous diseases as heart diseases, stroke, chronic obstructive pulmonary diseases, cancer and pneumonia. The built environment, in fact, alters the atmospheric air motion and can cause the trapping of pollutants inside the spaces between buildings instead of their dispersion (Kurppa et al., 2018 [3]).

The urban canopy can be classified in different ways, but usually the urban canyon (two linear buildings separated by a street) with its geometrical descriptors is the most commonly employed elementary block to describe the built environment, in particular now that individual urban canyons with their descriptors can be extracted on large extensions of real cities via free online available Geographic Information System (GIS) data (see, e.g., Salvadori et al., 2019 [4], Badas et al., 2019, [5], Salvadori et al., 2021-a [6], Salvadori et al., 2021-b [7]).

The study of the classification of elementary blocks of the boult environment can be called as a parametric study: the parametric study of the influence of urban blocks in pollutant dispersion has been a key element in the simulation via CFD (Computational Fluid Dynamics) for urban planning processes (da Silva et al., 2021-a [8], Costabile et al., 2006-a [9] and 2006-b [10]). Several authors investigated the pollutant dispersion in a single block or in a combination of blocks. Di Bernardino et al. (2017 [11]) investigated in a water channel the dispersion of a pollutant, emitted from three different point sources, around an isolated, cubic obstacle. Yassin (2011 [12]) have investigated via numerical simulations the impact of height and shape of building roof on the air quality in two-dimensional urban street canyons where the release of a pollutant was at the street level. Ferrari et al. (2019 [13]) performed, in the water tunnel, a similar experiment but with the release of the pollutant from a chimneystack. To study the pollutant dispersion, they employed a non-intrusive and quasi-continuous-in-space Digital Image Analysis technique (see Ferrari, 2017 [14], for a review) to measure the concentration, the Laser Induced Fluorescence technique employed in [15], [16] and [17]. Nosek et al. (2017 [18]) have investigated in a wind tunnel the impact of roof height non-uniformity on pollutant dispersion among groups of courtyard buildings and street intersections, with the pollutant released at the street level. Hall et al. (1999 [19]) studied in a laboratory wind tunnel the dispersion of a pollutant released from a point source at the courtyard floor level in courtyards and other enclosed buildings.

Among the blocks, the courtyard building (a building with an unroofed internal area) is one of the typical block establishing the urban environment shape, and it is also one of the most common, in particular in Europe (da Silva et al., 2021-b [20], Taleghani et al., 2014 [21]) but not only. As a matter of fact, the courtyard buildings are also very common in hot and arid climatic areas, because of their thermal efficiency (Chiri et al., 2020 [22], Al-Hafith et al., 2017 [23], Cantón et al., 2014 [24]).

* Corresponding author: ferraris@unica.it

As can be seen from the above quoted papers, most of the investigations of pollutant dispersion in the built environment are often carried on with the release of the pollutant from a street or a floor of the modelled building, in order to simulate traffic pollution. Less common is the release from a chimneystack, even if recent investigations highlight its relevance in the urban air quality issues (see, among the others, by Paunu et al., 2021 [25], Huy et al., 2021 [26] and Suryati et al., 2021 [27]). In none of those investigations, anyway, the chimneystacks were on a courtyard building.

For this reason, as, on the best of the author knowledge, the dispersion of a plume of pollutant emitted from a chimneystack above the roof of courtyard in a group of courtyards has been never investigated, the target of this paper is to fill this gap via a parametric study through numerical simulation with the software ENVI-met (see Section 2) on a group of four identical courtyards, where the length of the courtyard, i.e. the perpendicular-to-the-wind dimension of the internal open space of the building, is the variable parameter, while all the other parameters are kept constant. Among the others, the target here is also to evaluate if and how much the pollutant released form a chimneystack on a courtyard building can affect the internal courtyards of downstream buildings as well as the streets among the buildings.

2 Materials and methods

The ENVI-met software (Bruse and Fleer, 1998 [28]), able to model, among the others, the turbulence and pollutant dispersion in the built environment, has been employed in this work. ENVI-met has been widely employed for urban microclimate simulation (see the list of papers reported in Fabbri and Costanzo, 2020 [29]), as well as for the investigation of pollutant dispersion in the built environment. For instance, Nasrollahi et al (2017 [30]) employed ENVI-met to investigate the thermal performance of courtyards of different configurations, typical of Shiraz, in Iran. Among the others, also Wu et al., 2021 [31], Viecco et al., 2021 [32], Sun et al., 2021 [33], Jing and Liang 2021 [34] and Xing and Brimblecombe 2019 [35] employed ENVI-met to simulate the pollutant dispersion in several different urban configurations.

The modelled built environment is composed by (see Figure 1, where the names of the courtyards and of the streets are also reported) four identical courtyards buildings, with a constant height (10 m), a constant thickness (10 m), a constant courtyard width (W = 5 m where W is the courtyard dimension parallel to the wind direction), a constant width of the streets (i.e. a constant distance between the buildings, 10 m) and a variable courtyard length (L = 5 m, 10 m, 15 m, and 20 m, where L is the courtyard dimension perpendicular to the wind direction), and a 2m-height chimneystack on the roof of courtyard 1 (highlighted with the red dot on Figure 1) releasing a constant flow rate of carbon monoxide CO (that, consequently, is released form a point source). This arrangement was chosen as being typical of some family houses in the residential areas of many Italian towns. Anyway, it should be recalled that the target of this work is a parametric investigation on the influence of the relative dimensions of courtyard, building and road dimension on the capability to disperse the pollutant released from a chimneystack and not to simulate what happens in a portion of a real town. The configurations simulated where named W5L05, W5L10, W5L15 and W5L20.

The simulated wind is constant and from the East-direction, with an undisturbed velocity U_0 of 2.3 m/s and an air temperature of 19.8°C at the beginning of the simulation, i.e. at 6 a.m. of the 23/06/2018 (data taken from the meteorological station of Rome/Ciampino, Italy).

The domain is 250 cells-long x 150-180 cells-wide x 60 cells-height, with the single cell being a 1m-side cube. The difference in the width of the domain is due to the variable dimension of the courtyards. The domain size has been chosen to left enough space around the buildings for the flow to reattach after the detachment due to the presence of the building and to allow the stability to the numerical code (according to Blocken, 2015 [36]). The first cell close to the terrain is divided by the code into five smaller cells, in order to better simulate the typical boundary layer developing close to the terrain. Moreover, ENVI-met generates a logarithmic wind profile, typical of the Urban Boundary Layer, according to the given input data and the specific location and season. ENVI-met simulates the air turbulence via the so-called 2-equation Turbulence Kinetic Energy (TKE) Model, i.e. numerically solving the Kinetic Energy (KE) balance equation (describing the distribution of KE depending on its production, advection, diffusion and destruction) together with the Dissipation Rate of TKE (ε) equation.

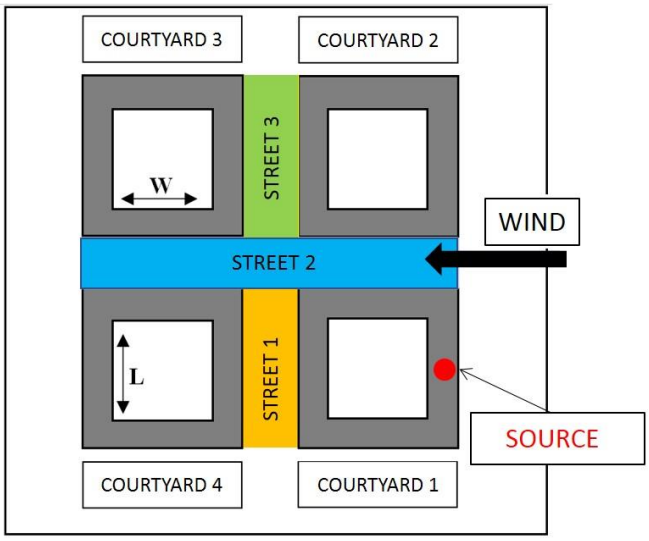

Fig. 1. Sketch of the group of courtyards, with the relevant dimensions, the pollutant source location, the wind direction, the names of the courtyards and the names of the streets.

3 Results

In Figure 2, the horizontal field of non-dimensional pollutant concentration C/C_0 (i.e., the pollutant concentration reduction, as C_0 is the CO concentration at the chimneystack outlet, i.e. the maximum concentration in the domain), extracted on the plane at the building roof height, is shown: colours close to the yellow point out where the concentration is higher, while colours close to the blue indicates where the concentration is almost zero. The white vectors represent the velocity direction (arrow) and magnitude (length). For the sake of clarity, not the whole domain is shown but only a zoom in the closest region to the courtyards where the flow is biased by the presence of the buildings. It is visible that the pollutant enters the courtyard C.1, the one upstream, but also the courtyard C.4, the one downstream, as well as the street 1, the one between C.1 and C.4, and downstream the courtyard C.4. On the contrary, in the courtyards C.2 e C.3 the pollutant does not enter. In particular, the pollutant concentration reduction C/C_0 in the courtyard C.1 is around 0.040, in the courtyard C.4 around 0.010 and in the street 1 around 0.015, with values close to the zero in the courtyards C.2 e C.3. The CO non-dimensional concentration in the street 1 is around 0.010, around 0.005 in the street 2 and almost zero in the street 3.

On Figure 3, the vertical field of non-dimensional pollutant concentration C/C_0, in colours, as well as the velocity vectors (white arrows) at the middle section of courtyards 1 and 4 are shown. Similar considerations as the ones for Figure 2 can be drawn.

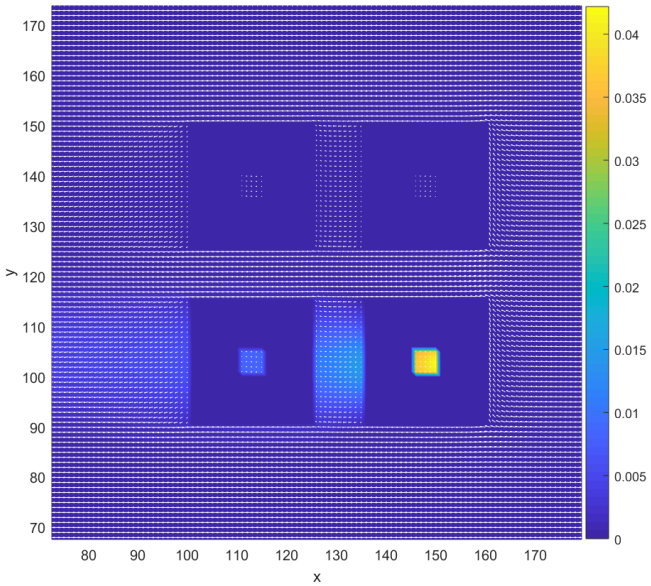

Fig. 2. Horizontal field of nondimensional CO concentration C/C_0 at the roof level (wind comes from the right).

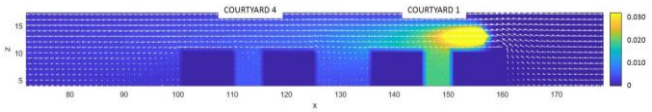

Fig. 3. Vertical field of nondimensional CO concentration C/C_0 at the middle section of courtyards 1 and 4 (wind comes from the right).

To quantify the effect of the simulated group of four courtyards and of their dimensions in reducing the pollutant penetration in the inner courtyards the non-dimensional maximum CO concentration C_{MAX}/C_0 inside the four courtyards, for the different simulated courtyard dimensions, in the volume inside the courtyard buildings is plotted, for each one of the four configurations, versus the hours of the day on Figures from 4 to 7. In the x-axis, the hours of the day are from 7 a.m. of the first simulated day to 6 a.m. of the following day. Similarly, on Figures from 8 to 10 the non-dimensional maximum CO concentration C_{MAX}/C_0 inside the three streets, for the different simulated courtyard dimensions, is plotted, for each one of the four configurations, versus the hours of the day; in this case, the concentration is measured at a 2 m height on the street level, i.e. at pedestrian level. In all the Figures from 4 to 10, the case W5L05 is represented by a continuous black line with black circles, the case W5L10 is represented by a dashed blue line with blue plus, the case W5L15 is represented by a continuous red line with red asterisks and the case W5L20 is represented by a dashed green line with green circles. The minimum non-dimensional concentration inside the courtyards is not shown, because it is always and everywhere almost zero.

Figures from 4 to 10 clearly show a time dependency due to the variable sunlight warming during the day which, in turn, increases the turbulent stirring during the warmest hours of the day.

On Figure 4 and 5, the non-dimensional maximum CO concentration C_{MAX}/C_0 inside the courtyards C.1 and C.4, for the different simulated courtyard dimensions, in the volume inside the courtyard buildings is plotted for each one of the four configurations, versus the hours of the day. The two courtyards show a similar trend, but with very different values, higher in the C.1 (as expected, because is the one where the chimneystack is located) and lower in the C.4. Moreover, for both the courtyards the concentration increases as the volume decreases and tends to have the highest value at 7 a.m., to then decrease until 1 p.m., increase until 9 p.m. and then remain almost constant until the end of the simulated day. This is due to the variation of the irradiation during the day, so during the warmer hours of the day when there is a higher temperature of the air volume close to the ground, which causes a reduction of the air density and an increase of the turbulent stirring which, in turns, favor the dilution of the pollutant.

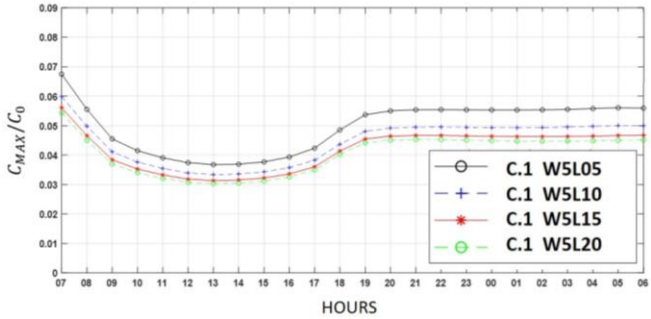

Fig. 4. Daily variation of the nondimensional maximum CO concentration C_{MAX}/C_0 inside the courtyard 1, for the different simulated courtyard dimensions.

On Figure 6 and 7, the non-dimensional maximum CO concentration C_{MAX}/C_0 inside the courtyards C.2 and C.3, for the different simulated courtyard dimensions, in the volume inside the courtyard buildings is plotted for each one of the four configurations, versus the hours of the day. As for the C.1 e C.4, the two courtyards show a similar trend, but with very different values, higher in the C.3 (that results downstream to the chimneystack) and lower in the C.4 (that results perpendicular to the chimneystack). Moreover, for both the courtyards the concentration increases as the volume decreases and it is almost zero from 6 p.m. to 8 a.m., to then increase until 1 p.m., where the highest value is found.

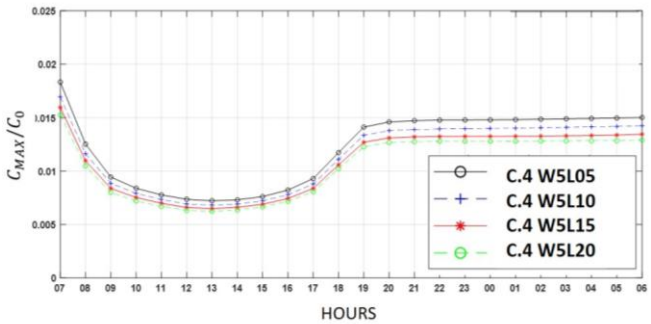

Fig. 5. Daily variation of the nondimensional maximum CO concentration C_{MAX}/C_0 inside the courtyard 4, for the different simulated courtyard dimensions.

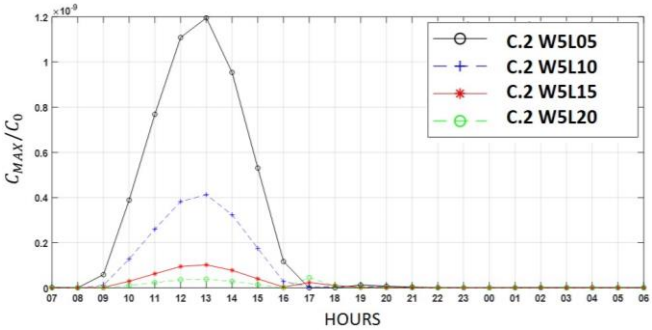

Fig. 6. Daily variation of the nondimensional maximum CO concentration C_{MAX}/C_0 inside the courtyard 2, for the different simulated courtyard dimensions.

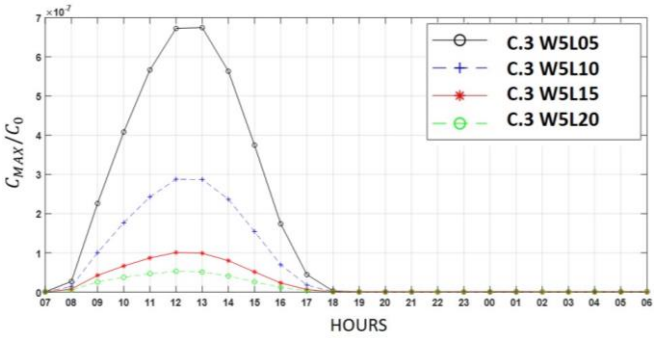

Fig. 7. Daily variation of the nondimensional maximum CO concentration C_{MAX}/C_0 inside the courtyard 3, for the different simulated courtyard dimensions.

On Figure 8, the daily variation of the nondimensional maximum CO concentration C_{MAX}/C_0 inside the street 1, for the different simulated courtyard dimensions, is reported. The pollutant trend is the same for all the simulated configurations, without a significative dependence on the courtyard dimension. The trend is very similar to the one of C.1 and C.4 and with values that are not negligible and similar to the one of the courtyard 4.

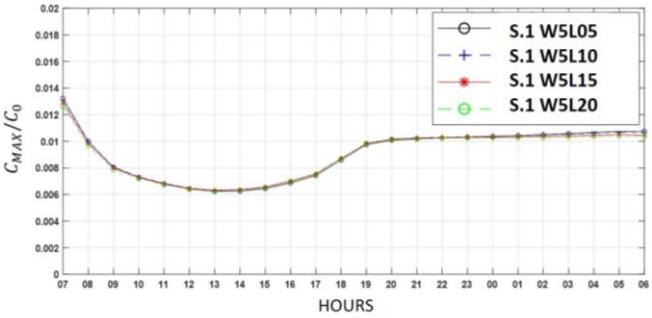

Fig. 8. Daily variation of the nondimensional maximum CO concentration C_{MAX}/C_0 inside the street 1, for the different simulated courtyard dimensions.

On Figure 9, the daily variation of the nondimensional maximum CO concentration C_{MAX}/C_0 inside the street 2, for the different simulated courtyard dimensions, is reported. The pollutant trend is the same for all the simulated configurations, with increasing values as the courtyard dimension decreases.

Eventually, on Figure 10, the daily variation of the nondimensional maximum CO concentration C_{MAX}/C_0 inside the street 3, for the different simulated courtyard dimensions, is reported. The trend is very similar to the one of C.2 and C.3, with values that higher than the ones of the quoted courtyards and with increasing values as the courtyard dimension decreases.

In summary, the results show, among the others, how the pollutant emitted from an upstream building can harm also the downstream buildings and the streets close to the buildings, with an increasing concentration as the courtyard volume decreases.

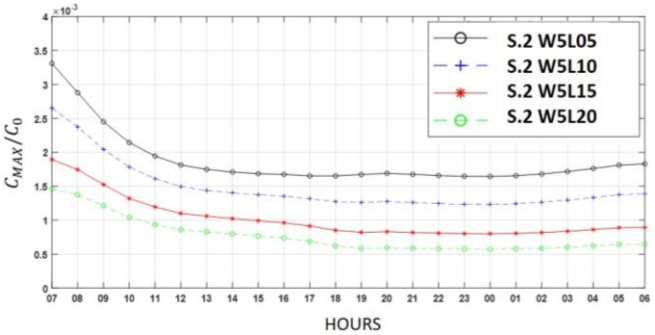

Fig. 9. Daily variation of the nondimensional maximum CO concentration C_{MAX}/C_0 inside the street 2, for the different simulated courtyard dimensions.

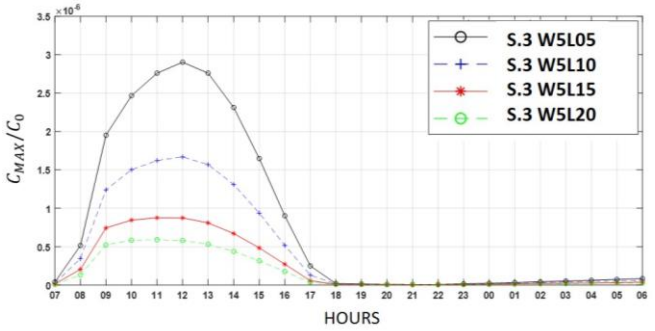

Fig. 10. Daily variation of the nondimensional maximum CO concentration C_{MAX}/C_0 inside the street 3, for the different simulated courtyard dimensions.

4 Conclusions

In this paper, the dispersion of a plume of pollutant emitted from a chimneystack above the roof of courtyard in a group of courtyards has been investigated, via a parametric study through numerical simulation with the software ENVI-met. The group consists of four identical courtyards, with a variable length of the courtyard, i.e. the perpendicular-to-the-wind dimension of the internal open space of the building, while all the other parameters are kept constant.

The main results are that the pollutant emitted from an upstream building can harm also the downstream buildings and the streets close to the buildings and, of course, the people living or working there. Moreover, the concentration tends to decrease as the courtyard volume increases, confirming the capability of the shape and dimensions of the courtyard building in contributing to the reduction of the pollutant concentration.

References

[1] World Health Organization, WHO global air quality guidelines: particulate matter (PM2.5 and PM10), ozone, nitrogen dioxide, sulfur dioxide and carbon monoxide. Executive summary. United nations, 2021.

[2] United Nations, '2018 Revision of World Urbanization Prospects'. 2018.

[3] M. Kurppa, A. Hellsten, M. Auvinen, S. Raasch, T. Vesala, and L. Järvi, 'Ventilation and Air Quality in City Blocks Using Large-Eddy Simulation—Urban Planning Perspective', Atmosphere, vol. 9, no. 2, p. 65, Feb. 2018, doi: 10.3390/atmos9020065.

[4] L. Salvadori et al., 'Similar urbanistic typologies and morpho-metric parametrization: Analysis of a possible date of construction based classification', presented at the 19th International Conference on Harmonisation within Atmospheric Dispersion Modelling for Regulatory Purposes, Harmo 2019; Bruges; Belgium; 3 June 2019 through 6 June 2019, 2019.

[5] M. G. Badas, L. Salvadori, M. Garau, G. Querzoli, and S. Ferrari, 'Urban areas parameterisation for CFD simulation and cities air quality analysis', IJEP, vol. 66, no. 1/2/3, p. 5, 2019, doi: 10.1504/IJEP.2019.104514.

[6] L. Salvadori, M. G. Badas, A. Di Bernardino, G. Querzoli, and S. Ferrari, 'A Street Graph-Based Morphometric Characterization of Two Large Urban Areas', Sustainability, vol. 13, no. 3, p. 1025, Jan. 2021, doi: 10.3390/su13031025.

[7] L. Salvadori, A. Di Bernardino, G. Querzoli, and S. Ferrari, 'A Novel Automatic Method for the Urban Canyon Parametrization Needed by Turbulence Numerical Simulations for Wind Energy Potential Assessment', Energies, vol. 14, no. 16, p. 4969, Aug. 2021, doi: 10.3390/en14164969.

[8] F. Trindade da Silva et al., 'Atmospheric dispersion and urban planning: An interdisciplinary approach to city modeling', Sustainable Cities and Society, vol. 70, p. 102882, Jul. 2021, doi: 10.1016/j.scs.2021.102882.

[9] F. Costabile, F. Wang, W. Hong, F. Liu, and I. Allegrini, 'CFD modelling of traffic-related air pollutants around an urban street-canyon in Suzhou', in Air Pollution XIV, The New Forest, UK, May 2006, vol. 1, pp. 297–306. doi: 10.2495/AIR06030.

[10] F. Costabile, F. Wang, W. Hong, F. Liu, and I. Allegrini, 'Spatial Distribution of Traffic Air Pollution and Evaluation of Transport Vehicle Emission Dispersion in Ambient Air in Urban Areas', JSME Int. J., Ser. B, vol. 49, no. 1, pp. 27–34, 2006, doi: 10.1299/jsmeb.49.27.

[11] A. D. Bernardino, P. Monti, G. Leuzzi, F. Sammartino, and S. Ferrari, 'Experimental investigation of turbulence and dispersion around an isolated cubic building', HARMO 2017 - 18th International Conference on Harmonisation within Atmospheric Dispersion Modelling for Regulatory Purposes, Proceedings, pp. 460–464, 2017.

[12] M. F. Yassin, 'Impact of height and shape of building roof on air quality in urban street canyons', Atmospheric Environment, vol. 45, no. 29, pp. 5220–5229, Sep. 2011, doi: 10.1016/j.atmosenv.2011.05.060.

[13] S. Ferrari, M. G. Badas, M. Garau, L. Salvadori, A. Seoni, and G. Querzoli, 'On The Effect Of The Shape Of Buildings And Chimneystacks On Ventilation And Pollutant Dispersion', EPJ Web Conf., vol. 213, p. 02017, 2019, doi: 10.1051/epjconf/201921302017.

[14] S. Ferrari, 'Image analysis techniques for the study of turbulent flows', EPJ Web of Conferences, vol. 143, p. 01001, 2017, doi: 10.1051/epjconf/201714301001.
[15] S. Ferrari and G. Querzoli, 'Laboratory experiments on the interaction between inclined negatively buoyant jets and regular waves', EPJ Web of Conferences, vol. 92, p. 02018, 2015, doi: 10.1051/epjconf/20159202018.
[16] S. Ferrari, M. Badas, and G. Querzoli, 'On the Effect of Regular Waves on Inclined Negatively Buoyant Jets', Water, vol. 10, no. 6, p. 726, Jun. 2018, doi: 10.3390/w10060726.
[17] S. Ferrari, M. G. Badas, and G. Querzoli, 'A non-intrusive and continuous-in-space technique to investigate the wave transformation and breaking over a breakwater', EPJ Web of Conferences, vol. 114, p. 02022, 2016, doi: 10.1051/epjconf/201611402022.
[18] Š. Nosek, L. Kukačka, K. Jurčáková, R. Kellnerová, and Z. Jaňour, 'Impact of roof height non-uniformity on pollutant transport between a street canyon and intersections', Environmental Pollution, vol. 227, pp. 125–138, Aug. 2017, doi: 10.1016/j.envpol.2017.03.073.
[19] D. J. Hall, S. Walker, and A. M. Spanton, 'Dispersion from courtyards and other enclosed spaces', Atmospheric Environment, vol. 33, no. 8, pp. 1187–1203, Apr. 1999, doi: 10.1016/S1352-2310(98)00284-2.
[20] F. Trindade da Silva, N. C. Reis, J. M. Santos, E. V. Goulart, and C. Engel de Alvarez, 'The impact of urban block typology on pollutant dispersion', Journal of Wind Engineering and Industrial Aerodynamics, vol. 210, p. 104524, Mar. 2021, doi: 10.1016/j.jweia.2021.104524.
[21] M. Taleghani, M. Tenpierik, and A. van den Dobbelsteen, 'Energy performance and thermal comfort of courtyard/atrium dwellings in the Netherlands in the light of climate change', Renewable Energy, vol. 63, pp. 486–497, Mar. 2014, doi: 10.1016/j.renene.2013.09.028.
[22] G. M. Chiri, M. Achenza, A. Canì, L. Neves, L. Tendas, and S. Ferrari, 'The Microclimate Design Process in Current African Development: The UEM Campus in Maputo, Mozambique', Energies, vol. 13, no. 9, p. 2316, May 2020, doi: 10.3390/en13092316.
[23] O. Al-Hafith, S. B K, S. Bradbury, and P. de Wilde, 'The Impact of Courtyard parameters on its shading level An experimental study in Baghdad, Iraq', Energy Procedia, vol. 134, pp. 99–109, Oct. 2017, doi: 10.1016/j.egypro.2017.09.539.
[24] M. A. Cantón, C. Ganem, G. Barea, and J. F. Llano, 'Courtyards as a passive strategy in semi dry areas. Assessment of summer energy and thermal conditions in a refurbished school building', Renewable Energy, vol. 69, pp. 437–446, Sep. 2014, doi: 10.1016/j.renene.2014.03.065.
[25] V.-V. Paunu et al., 'Spatial distribution of residential wood combustion emissions in the Nordic countries: How well national inventories represent local emissions?', Atmospheric Environment, vol. 264, p. 118712, Nov. 2021, doi: 10.1016/j.atmosenv.2021.118712.
[26] L. N. Huy, E. Winijkul, and N. T. Kim Oanh, 'Assessment of emissions from residential combustion in Southeast Asia and implications for climate forcing potential', Science of The Total Environment, vol. 785, p. 147311, Sep. 2021, doi: 10.1016/j.scitotenv.2021.147311.
[27] I. Suryati, R. Zulkarnain, and A. Pratama, 'Analysis of PM10 dispersion models from coal-fired power plant activities in North Sumatera by using CALPUFF', IOP Conf. Ser.: Earth Environ. Sci., vol. 802, no. 1, p. 012033, Jun. 2021, doi: 10.1088/1755-1315/802/1/012033.
[28] M. Bruse and H. Fleer, 'Simulating surface-plant-air interactions inside urban environments with a three dimensional numerical model', Environmental Modelling and Software, vol. 13, no. 3–4, pp. 373–384, 1998, doi: 10.1016/S1364-8152(98)00042-5.
[29] K. Fabbri and V. Costanzo, 'Drone-assisted infrared thermography for calibration of outdoor microclimate simulation models', Sustainable Cities and Society, vol. 52, p. 101855, Jan. 2020, doi: 10.1016/j.scs.2019.101855.
[30] N. Nasrollahi, M. Hatami, S. R. Khastar, and M. Taleghani, 'Numerical evaluation of thermal comfort in traditional courtyards to develop new microclimate design in a hot and dry climate', Sustainable Cities and Society, vol. 35, pp. 449–467, Nov. 2017, doi: 10.1016/j.scs.2017.08.017.
[31] J. Wu, K. Luo, Y. Wang, and Z. Wang, 'Urban road greenbelt configuration: The perspective of PM2.5 removal and air quality regulation', Environment International, vol. 157, p. 106786, Dec. 2021, doi: 10.1016/j.envint.2021.106786.
[32] M. Viecco, H. Jorquera, A. Sharma, W. Bustamante, H. J. S. Fernando, and S. Vera, 'Green roofs and green walls layouts for improved urban air quality by mitigating particulate matter', Building and Environment, vol. 204, p. 108120, Oct. 2021, doi: 10.1016/j.buildenv.2021.108120.
[33] D. (Jian) Sun, S. Wu, S. Shen, and T. Xu, 'Simulation and assessment of traffic pollutant dispersion at an urban signalized intersection using multiple platforms', Atmospheric Pollution Research, vol. 12, no. 7, p. 101087, Jul. 2021, doi: 10.1016/j.apr.2021.101087.
[34] L. Jing and Y. Liang, 'The impact of tree clusters on air circulation and pollutant diffusion-urban micro scale environmental simulation based on ENVI-met', IOP Conf. Ser.: Earth Environ. Sci., vol. 657, p. 012008, Feb. 2021, doi: 10.1088/1755-1315/657/1/012008.
[35] Y. Xing and P. Brimblecombe, 'Role of vegetation in deposition and dispersion of air pollution in urban parks', Atmospheric Environment, vol. 201, pp. 73–83, Mar. 2019, doi: 10.1016/j.atmosenv.2018.12.027.
[36] B. Blocken, 'Computational Fluid Dynamics for urban physics: Importance, scales, possibilities, limitations and ten tips and tricks towards accurate and reliable simulations', Building and Environment, vol. 91, pp. 219–245, Sep. 2015, doi: 10.1016/j.buildenv.2015.02.015.